Indian J Phys
https://doi.org/10.1007/s12648-020-01887-0

ORIGINAL PAPER

First-principles calculations of vibrational and optical properties of half-Heusler NaScSi

I Kars Durukan* and Y Oztekin Ciftci

Department of Physics, Faculty of Science, Gazi University, 06500 Ankara, Turkey

Received: 22 September 2019 / Accepted: 09 June 2020

Abstract: Ab initio calculation of the structural, mechanical, dynamic, thermodynamic, electronic, and optical properties of cubic half-Heusler compound NaScSi have been reported using density functional theory. Generalized gradient approximation has been used as the exchange and correlation potential for investigating these properties. The lattice constant, bulk modulus, the first pressure derivative of bulk modulus, and band gap of NaScSi have been calculated and compared to the previous XScSi (X = Na, Li, Ag, K) studies. The band structure and corresponding density of states have also been determined and analyzed. The elastic properties of the compound, calculated by the strain–stress method, satisfy the mechanical stability conditions for a cubic structure. According to the data obtained from the vibration properties, the compound is also stable dynamically. Additionally, heat capacity, entropy, and free energy of NaScSi have been calculated by using the phonon frequencies. The optical investigation of the compound shows high reflectivity in the UV region of the photon energy.

Keywords: Half-Heusler compounds; Electronic properties; Optical properties; NaScSi

1. Introduction

Heusler compounds have been studied both experimentally and theoretically [1–4] since they were discovered. These compounds are an intermetallic class consisting of three elements in 1:1:1 (half-Heusler) or 2:1:1 (full-Heusler) stoichiometric ratios. In full-Heusler alloys, X is usually a transition metal, such as Cu, Fe, Ni, Co, Ru; Y is usually Mn, Cr, or V; and Z can be Al, Ga, Ge, Si, Sn in L_{21} structure [5]. For half-Heusler alloys, the general formula is XYZ, where X can be a transition or alkali metal element, Y is another transition metal element, typically Mn or Cr, and Z is a member of the group IV element or a pnictide [6]. The full-Heusler compound can crystallize in the L_{21} structure (space group *Fm-3m* with Cu_2MnAl prototype structure with or space group *F-43m* with Hg_2CuTi prototype structure), while the half-Heusler can crystallize in the C_{1b} structure (space group *F4-3m* with MgAgAs prototype structure) [7, 8].

Heusler compounds are generally magnetic intermetallic with face-centered cubic crystal structure. A lot of Heusler compounds show properties relevant to spintronics such as magnetoresistance, Hall effect, ferro-, anti-ferro-, and ferrimagnetism, half- and semi-metallicity, semiconductivity with spin filter's ability, superconductivity, and topological band structure [9]. Due to their electronic structure indicating half-metallicity, Heusler compounds exhibit significant research topics such as magneto-caloric, thermoelectric, and magnetic shape memory effects [9, 10].

On the other hand, half-Heusler alloys are used for optoelectronic applications such as thin-film solar cells or laser diodes [11–15]. Half-Heusler materials could be used as thermoelectric semiconductors [11–13], piezoelectric semiconductors [14], optoelectronic semiconductors [15], and topological insulators [16, 17]. Because of possessing 100% spin polarization at the Fermi level and relatively high Curie temperature [18, 19], Heusler-based half-metals have attracted important interest for spintronics applications [20, 21]. Half-metals are considered ideal electrode materials for magnetic tunnel junctions [22], and giant magnetoresistance devices [23] for injecting spin-polarized currents in semiconductors [24].

The properties of many Heusler compounds can be easily estimated by valence electron concentration (VEC) [25]. Since the verification of the spin structure is experimentally difficult, the electronic structure calculation plays

*Corresponding author, E-mail: ilknurdurukan@gazi.edu.tr

Published online: 26 October 2020

© 2020 IACS

a vital role in the investigation of these compounds. Therefore, many researchers working both theoretically and experimentally have made great efforts to discover new Heusler compounds [26–29].

Several XScSi-based full-Heusler alloys were theoretically studied by Ciftci and Evecen [30] with a detailed analysis of the structural, mechanical, electronic, dynamic, and optical properties of MgAgAs-based LiScSi compound using the ab initio method. Kacimi et al. [31] performed a series of studies on the half-Heusler, considering structural, electronic, and optical properties of XScSi (X = Li, K, Na). Durukan and Ciftci [27] reported a detailed first-principle calculation to study the elastic anisotropy, vibrational, and optic properties of the AgScSi compound under pressure using GGA method with the projector augmented wave (PAW) method.

Elastic constants of crystals determine the stability for understanding the macroscopic mechanical properties of a material, which is the main parameter in material processing. Sound velocities and Debye temperature, which can also be determined by elastic constants, are the basic physical parameters of any material for thermal properties. Similarly, vibrational properties play a vital role to determine different properties of materials such as thermal conductivity, optical and phonon band gaps, specific heat, thermal expansions, and dynamical stability. Also, the electronic properties of the materials are very important in terms of determining the electrical conductivity, band structure, DOS, chemical bonding, and quality of the materials. On the other hand, the optical properties of solids provide an important tool for studying energy band structure, impurity levels, excitons, localized defects, lattice vibrations, and certain magnetic excitations [32, 33].

Up till now, to the best of our knowledge, there is no detailed theoretical work of the NaScSi compound about mechanical, vibrational, and optical properties. To use NaScSi in technology, the physical properties of this compound should be investigated in detail. So, this is a motivation to study and compare structural, mechanical, dynamic, thermodynamic, electronic, and optical properties of half-Heusler compound NaScSi to check its feasibility for optoelectronic devices such as detectors and lasers.

2. Method of calculation

All the calculations such as geometrical optimization and self-consistent calculations have been performed using the plane-wave pseudo-potential DFT method [32–36] implemented in the Vienna ab initio simulation package (VASP) within PAW method to obtain ground state structure [34, 37–39]. Within the generalized gradient approximation (GGA), we have used the Perdew–Burke–Ernzerhof parameterization (PBE) for the exchange–correlation functional [40]. The convergent threshold of the total energy and forces acting on every atom is set to 10^{-8} and 0.0001 eV/A, respectively. The plane-wave basis sets with energy cutoff are set to 700 eV and Brillouin zone integrations, using 15 × 15 × 15 Monkhorst and Pack [41] *k*-points in the irreducible zone for NaScSi. Pressure on the cell is minimized within the constraint of the constant volume. Based on the optimized structure, other properties are calculated. The elastic properties are exploited to estimate using the stress–strain method [30] by the aid of IBRION = 6 commands implemented in VASP 5.4. For the analysis of vibrational properties, we have used the 2 × 2 × 2 supercells to calculate the phonon frequencies. Real-space force constants are calculated by the density functional perturbation theory applied in the VASP code. PHONOPY code is used to calculate phonon frequencies [42]. Finally, Debye model [43–46] has been applied to calculate the thermodynamic properties of NaScSi compound.

3. Results and discussion

3.1. Structural properties

The analysis of structural properties is the most important parameter for determining the behavior of some materials. Half-Heusler NaScSi has a cubic crystal structure which is MgAgAs prototype structure (space group: *F4-3m*/No. 216). The unit cell of NaScSi is shown in Fig. 1. There are three atoms in the unit cell where the Wyckoff atomic positions are occupied by 4b site (0.5, 0.5, 0.5), 4c site (0.25, 0.25, 0.25), and 4a site (0.0, 0.0, 0.0) for Na, Sc, and Si, respectively [47]. Here, geometry optimization is

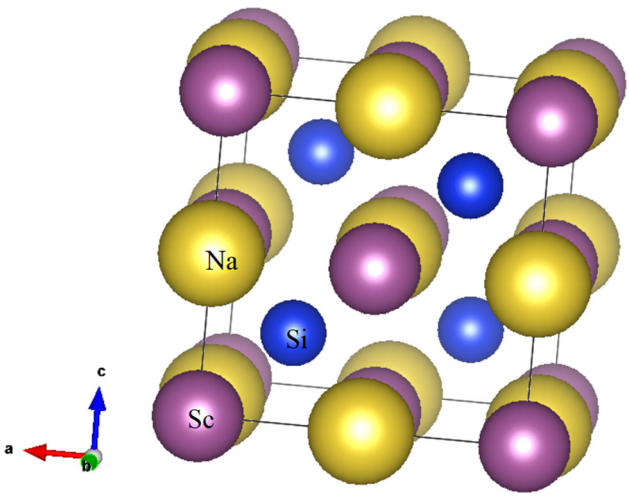


Fig. 1 The unit cell of NaScSi

performed on the primitive cell of NaScSi including three atoms using VASP. To perform the optimization process, we have relieved the volume of the unit cell and all atomic positions (ISIF = 3 in VASP). Our results have been fitted to the Murnaghan state equation [48] to obtain bulk modulus (B) and the first derivative of the bulk module (B'). The obtained results of the investigated compound are given in Table 1 and compared with the other theoretical result and XScSi (X: Li, Na, K, and Ag) compounds. It is seen from Table 1 that our calculated lattice constant of NaScSi (a = 6.598 Å) structure is in good agreement with the theoretical study [31] (a = 6.605 Å). There is a 0.1% difference between the lattice constant values of our study and another theoretical study [31]. These calculated lattice constant values exhibit the reliability of the method used in our calculations. It is well known that GGA generally overestimates the lattice parameter. While all parameters have been calculated by VASP code in our calculation, Wien2k code was used in the other theoretical study.

Li, Na, and K are in the same group on the periodic table and have similar chemical properties. The atomic radius of Li, Na, and K is 1.45 Å, 1.80 Å, and 2.20 Å, respectively. As shown in Table 1, the lattice constants of the compounds are 6.264 Å for LiScSi [46], 6.598 for NaScSi (Å) [31], and 7.005 Å for KScSi [31]. As you can see, the atomic radius and the lattice constant are directly proportional to each other. The observed increment in the lattice parameter is related to the increase in the atomic radius in the same group. Although the atomic radius of Ag is between the atomic radius of Li and K, the lattice constant of AgScSi (6.226 Å) [27] is the smallest value. This may be because Ag is in different groups in the periodic table.

The bulk modulus measures how resistant a material is to compressibility while the pressure derivative of bulk modulus measures its response to a slight change in pressure. Our calculated bulk modulus value, 47.22 GPa, indicates that this compound could be easily compressed due to the small value of its bulk modulus. In the previous studies, the bulk module of LiScSi [30] and AgScSi [27] compounds was 54.71 GPa and 83.4 GPa, respectively. The bulk modulus values of Na, Ag, Li, and K were 6, 36, 100, and 3 GPa, respectively. This explains the difference in the bulk module in the compounds. As a result, NaScSi is a softer compound than other compounds. The obtained pressure derivative of the bulk modulus (B') is 3.99 for NaScSi. This value is smaller than that of AgScSi [27]. Thus, NaScSi is more resistant to pressure than AgScSi. There is no value for bulk modulus and its first derivative for NaScSi to compare with the literature. Thus, these results are the predictions.

As shown in Table 1, the band gap value (0.619 eV), which will be discussed in detail in the Electronic Properties section, is very compatible with the result of the other theoretical work (0.639 eV) [31]. Although there is no experimental value of the band gap values for NaScSi, it is well known that the band gap value is generally underestimated due to limitations of the DFT.

3.2. Mechanical properties

Elastic constants give us important information due to the strength and stability of the materials and nature of the binding forces in solids. Important physical properties such as hardness, sound velocities, Debye temperature, shear modulus, and melting point can be calculated via elastic constants [49]. The elastic constants are second derivatives of the total energy concerning various lattice deformations. Thus, more complete calculations of the total energy are important for the elastic constants [50]. The number of independent elastic constants is generally reduced if the crystal has symmetry elements, and in the state of the cubic crystal, there are only three independent elastic constants. In the cubic crystals, three independent elastic constants C_{11}, C_{12}, and C_{44} are determined by using suitable lattice distortions [51].

The response of a crystal to applied external forces is determined by elastic constants; therefore, elastic constants provide significant information about the mechanical properties of materials. For example, structural stability, anisotropic characteristic, and bonding properties of materials can be determined by elastic constants [52].

The knowledge of elastic properties obtained with the strain–stress method can be used to analyze the structural stability and mechanical properties of the material. In particular, in the case of cubic crystals, the conditions of stability reduce to a very simple form: $C_{11} - C_{12} > 0$; $C_{11} + 2C_{12} > 0$; $C_{44} > 0$. These stability conditions are necessary and sufficient for elastic constants. The computed elastic constants are listed in Table 2. Our calculated elastic constants in the NaScSi compound obey the Born's stability criteria [53]. These stability criteria, which must be positive, give information about the strain energy when homogeneous elastic deformation is applied [54].

From the calculated C_{ij} values, bulk modulus B (GPa), shear modulus G (GPa), Young's modulus E (GPa), hardness Hv (GPa), plasticity measurement (B/C_{44}), G/B ratio, C_{11}–C_{44} Cauchy pressure (GPa), Poisson's ratio (υ), and Zener anisotropy factor (A) of NaScSi compound could be calculated as follows [55–58]:

$$B = \frac{1}{3}(C_{11} + 2C_{12}) \tag{1}$$

$$G = \frac{1}{5}(C_{11} - C_{12} + 3C_{44}) \tag{2}$$

Table 1 Lattice constant, bulk module, first pressure derivative of bulk module, and band gap of NaScSi

Material	a (Å)	Atomic radius (Å)	B (GPa)	B'	E_g (eV)
NaScSi (our study)	6.598	1.80	47.22	3.99	0.619
NaScSi (theory [31])	6.605				0.639
AgScSi [27]	6.226	1.60	83.4	4.391	0.439
LiScSi [30]	6.264	1.45	54.71		0.718
KScSi [31]	7.005	2.20			0.377

Table 2 Elastic constant of NaScSi

Material	C_{11}	C_{12}	C_{44}
NaScSi (our study)	86.9	28.3	18.0
LiScSi [30]	95.6	34.3	19.0
AgScSi [27]	140.9	54.7	36.8

$$E = \frac{9BG}{3B + G} \tag{3}$$

$$\upsilon = \frac{3B - 2G}{2(3B + G)} \tag{4}$$

$$A = \frac{2C_{44}}{C_{11} - C_{12}} \tag{5}$$

$$H_v = 2\left(\left(\frac{G}{B}\right)^2 G\right)^{0.585} - 3. \tag{6}$$

The calculated results are listed in Table 3. The strength of a material is determined by mechanical properties. The bulk modulus is a measure of the resistance of the material to volume change. The bulk modulus value calculated from elastic constant using Eq. (1) is 47.8 GPa, which is very close to the value calculated from Murnaghan's equation of state (47.22 GPa). The shear module is a measure of the resistance of the atom against the movement of the atomic planes. High shear modulus reflects covalent nature. Young's modulus can be used as a measure of the resistance of the material against elastic stretching. As shown in Table 3, NaScSi has low Young and shear modulus indicating soft material. The LiScSi and AgScSi compounds are also soft material due to their lower Young and shear modulus [27, 30]. Hardness is a parameter required to characterize the material. Vickers hardness can be calculated with the help of Eq. (6). As shown in Table 3, Vickers hardness values are 1.84 GPa for NaScSi, 1.56 GPa for LiScSi [30], and 4.025 GPa for AgScSi [27], indicating that XScSi (X = Na, Li, Ag) compounds are relatively soft. If the hardness value of the material is 10 GPa, the material is known as a hard material, and if this value is 40 GPa and above, it is known as super-hard material [59]. In material science, plasticity defines the deformation of a material (solid) which undergoes irreversible shape changes against the applied force. The ratio of bulk modulus (B) to C_{44} may be interpreted as a measure of the plasticity [60]. This ratio is also calculated and given in Table 3. The plasticity value of NaScSi compound is low, and those of the other AgScSi [27] and LiScSi [30] compounds are close to the plasticity of NaScSi. It is important to know whether the material is ductile or brittle in terms of its suitability in technology. The coefficient of the shear–bulk modulus (G/B) can be used to estimate the brittleness or ductile behavior of compounds. If this ratio is less than 0.57, materials are considered ductile; otherwise, they are fragile [61]. This ratio of NaScSi compound is found to be 0.456. Therefore, the compound shows a ductile character. The G/B ratio of LiScSi [30] and AgScSi [27] compounds is 0.421 and 0.468, respectively. These compounds are also ductile characters like NaScSi as shown in Table 3. The Cauchy pressure, defined as the difference between the two special

Table 3 Bulk modulus B (GPa), shear modulus G (GPa), Young's modulus E (GPa), hardness (GPa), plasticity measurement B/C_{44}, G/B ratio, C_{11}–C_{44} Cauchy pressure (GPa), Poisson's ratio (υ), and Zener anisotropy factor (A) of AgScX (X = Ge, C) compounds

Material	B	G	E	Hv	B/C_{44}	G/B	C_{12}–C_{44}	v	A
NaScSi (our study)	47.8	21.8	56.7	1.84	2.65	0.456	10.3	0.302	0.614
LiScSi [30]	54.716	23.059	60.66	1.56	2.87	0.421	15.244	0.315	0.620
AgScSi [27]	83.54	39.1	101.4	4.0:5	2.27	0.468	17.9	0.2972	1.001

elastic fixed C_{12}–C_{44}, is a second method used to determine the ductility and fragility. Ganesham et al. [62] have found a correlation between the binding properties and ductility. The binding character of the cubic compounds is described according to the pressure of Cauchy (C_{12}–C_{44}). The compounds with positive Cauchy pressure are metallic, whereas with negative Cauchy pressure, compounds form more angular or covalent bonds [63]. NaScSi, like LiScSi [30] and AgScSi [27], has ductile and metallic character due to its bonding properties. For another method, we can refer to Frantsevich [42], which distinguishes the ductility and fragility of materials due to their Poisson's ratio (v) values. The critical value of the Poisson's ratio for a material is 0.33 as $v < 0.33$ (> 0.33) indicates the brittle (ductile) character. As can be seen from Table 3, like LiScSi [30] and AgScSi [27], NaScSi has a ductile character due to its Poisson's ratio (v) value A, which is a measure of the degree of elastic anisotropy in solids and is important for engineering science, and it is given as:

$$A = \frac{2C_{44}}{C_{11} - C_{12}}. \tag{7}$$

In our work, NaScSi is anisotropic with the A value 0.614 as LiScSi [30]; on the other hand, AgScSi [27] is completely isotropic.

3.3. Vibrational properties

We have analyzed the phonon spectra of NaScSi compound for analysis of the vibrational properties, using a supercell finite displacement method implemented in the PHONOPY package [42] where a set of second-order force-constant matrices are obtained and used in VASP as the force constant calculator for phonon distribution calculations [64]. The supercell is used to obtain long-range force constants between atoms [65]. For these calculations, the second-order force constants are calculated using $2 \times 2 \times 2$ supercell expansions of the conventional *F4-3m* containing 24 atoms with the displacement step 0.02 A. We have found that this cell is sufficiently large to converge the shape of the phonon density of states to obtain a higher-quality dispersion. Phonon spectra with three atoms in the primitive cell have nine phonon branches, three of which are acoustic branches and the rest are optical branches. In the phonon dispersion curve, the high symmetry points ΓX, XK, KΓ, ΓL, LX, XW, and WL are used for the half-Heusler MgAgAs structure. As shown in Fig. 2, the NaScSi compound is dynamically stable because none of the branches involve a soft mode in the Brillouin zone. The general features are consistent with phonon dispersion relations reported for other HH compounds such as LiScSi [30] and AgScSi [27]. The sharp peaks in the DOS correspond to the flats in the phonon dispersion curve. From the partial DOS, it can be inferred that Na and Sc atoms contribute a major part to the modes with 0–6 THz. The modes > 7 THz are predominantly determined by the vibrations of the Na and Si atoms.

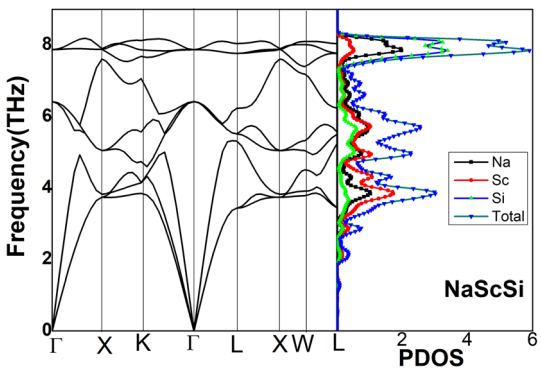


Fig. 2 Phonon frequencies and phonon partial density of states for NaScSi

The MgAgAs structure (space group *F4-3m*) of NaScSi exhibits T_d point group, and Wyckoff positions for Na, Sc, and Si atoms are 4c, 4a, and 4d, respectively. This T_d point group symmetry has three-dimensional (T_2) one irreducible representation. At Brillouin zone center Γ points, decomposition of vibrational representation into T_d group irreducible representation is shown as $\Gamma = 3T_2$. For the optical phonons, we can represent $\Gamma_{optic} = 2\ T_2$, while the acoustical phonons have the T_2 irreducible representation. As a result, the mode of T_2 is active in both Raman and IR spectra. Here, we did not take into effect LO–TO splitting. So, the frequencies of the two triply degenerate optical phonons are 6.416 and 7.854 THz, respectively.

Phonon dispersion curve plays a key parameter in dynamical behaviors and thermal properties such as constant volume heat capacity (C_v), Helmholtz free energy (F), entropy (S), and internal energy (E), given as [66]:

$$F = rk_B T \int_0^\infty g(\omega) \ln\left[2 \sin h\left(\frac{\hbar\omega}{2k_B T}\right)\right] d\omega \tag{8}$$

$$C_v = rk_B \int_0^\infty g(\omega) \left(\frac{\hbar\omega}{k_B T}\right)^2 \frac{\exp\left(\frac{\hbar\omega}{k_B T}\right)}{\left[\exp\left(\frac{\hbar\omega}{k_B T}\right) - 1\right]} d\omega \tag{9}$$

$$S = rk_B \int_0^\infty g(\omega) \left\{ \left(\frac{\hbar\omega}{2k_B T}\right) \left[\cot h\left(\left(\frac{\hbar\omega}{2k_B T}\right)\right) - 1\right] - \ln\left[1 - \exp\left(\frac{\hbar\omega}{2k_B T}\right)\right] \right\} d\omega \tag{10}$$

where $g(\omega)$ is phonon DOS and r is the degree of freedom for the unit cell.

In Fig. 3a, the graph of the contribution of the lattice to the heat capacity follows the Debye model and approaches

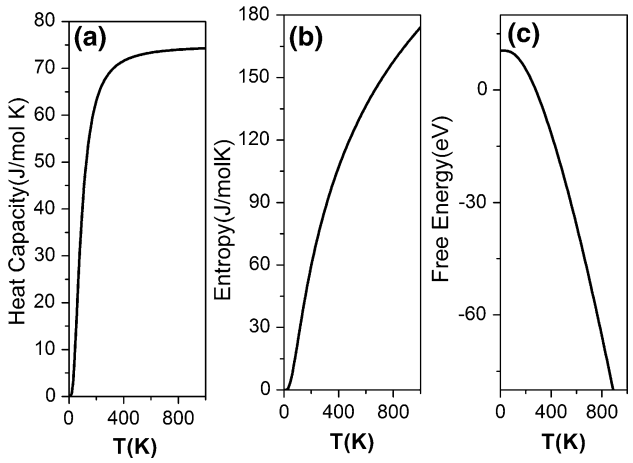


Fig. 3 (**a**) Heat capacity, (**b**) entropy, and (**c**) free energy versus temperature for NaScSi

the Dulong–Petit limit at high temperatures. In Fig. 3(b), entropy increases with temperature. On the contrary of Fig. 3a and Fig. 3b, the free energy decreases with the increasing temperature in Fig 3c.

3.4. Electronic properties

To analyze the suitability of the NaScSi compound for electronic devices, we have calculated the band structure along with the high-symmetry directions in the Brillouin zone. In Fig. 4, the band structure of the compound is presented where the Fermi energy level is fixed to zero. Figure 4a shows that the maximum valence band for our compound is at point X, whereas the conduction band extends at the minimum X-point, expressing a semiconductor character with a direct band gap.

The DOS of the system shows the number of states that are to be occupied by the system at each energy level. DOS has been represented mathematically as a distribution by a probability density function, and it is generally an average over the space and time domains of the various states occupied by the system. DOS calculations allow one to determine the general distribution of states as a function of energy.

The obtained band gap of NaScSi compound and other XScSi (X: Na, Li, Ag, and K) compounds data are listed in Table 1.

The total density and partial density of states are also plotted in Fig. 4b. The valence bands are located in three regions. The first region of the valence band consists of Si-*s* states. The second region originates from the hybridization of Sc-*d* states and Si-*p* states. In the third region of the conduction band, above the Fermi energy level, the major contribution comes from Sc *d*-states, and minor contribution comes from Si-*p*. In AgScSi [27] and LiScSi [30] compounds, the contribution of the total and partial density of states is similar to that of the NaScSi compound.

Charge density is an interesting measure for the investigation of the type of bonding among the constituent atoms of an alloy. Also, it gives an idea of the measurements of the feasibility of electron to be present at a particular position. Figure 5 shows the charge density plot of NaScSi in (100) plane, changing from 0.0 to 0.08 eA^{-3}. It can be seen from Fig. 5 that the charges are shared among the Na, Sc, and Si atoms, confirming covalent bonding between them. Moreover, the charge density distribution between cation and anion is spherical, indicating ionic bonding between them and consistent with similar half-Heusler compounds like CaAuBi [67].

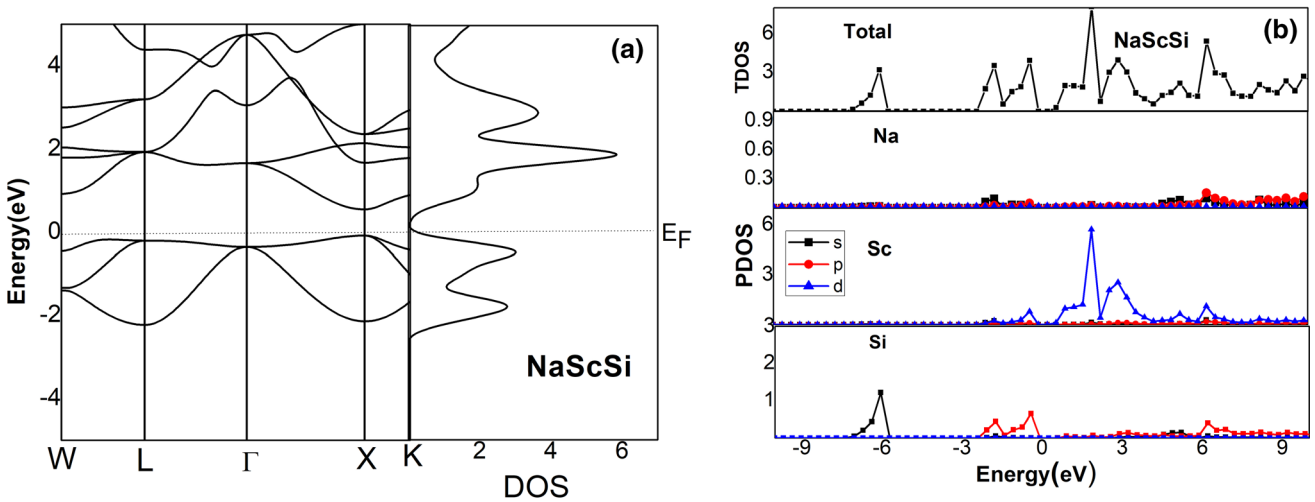


Fig. 4 (**a**) Electronic band structure and total density of states for NaScSi, (**b**) calculated partial density of states for NaScSi

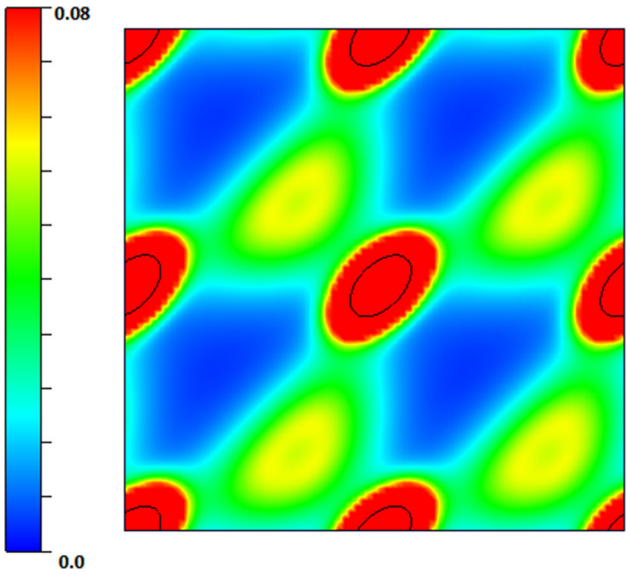


Fig. 5 2D charge density map for (100) plane for NaScSi

3.5. Optical properties

Optical properties have a crucial role in understanding the optoelectronic nature of a material. Furthermore, the optical property analysis is very important since semiconductors often exhibit a metal-like behavior at very low frequencies; on the contrary, they exhibit insulating behavior at very high frequencies [68]. The optical properties of the NaScSi compound are also determined and discussed. The results are shown in Fig. 4a–f. The complex dielectric function $\varepsilon(\omega)$ consists of two parts, the real and the imaginary, due to the response of the substance to the incoming light. This function $\varepsilon(\omega)$ is given by the following equation:

$$\varepsilon(\omega) = \varepsilon_1(\omega) + \varepsilon_2(\omega). \tag{11}$$

Here, $\varepsilon_1(\omega)$ and $\varepsilon_2(\omega)$ are the real and imaginary parts of the dielectric function related to the polarization and loss of energy, respectively.

Dielectric function is a complex function, providing calculations of the optical properties of materials. The linear response of a medium to external electrical and magnetic fields is measured by this function. Half-metals have the unique property of being as conductors in a particular spin channel and as semiconductors in the opposite spin channel. This half-metallic behavior produces electrical conduction, resulting from the charge carriers of a particular spin direction only. Spin polarization in half-metallic materials is 100%, generating spin-polarized current which helps in maximizing the efficiency of magneto-electronic devices. Since the half-metallic half-Heusler compounds have important magneto-optical properties, they have many applications like only one type of electrons, i.e., spin-up or spin-down, and, thus, be used as electrical switches. These properties make half-metals suitable for applications in spintronics [69].

The optical properties of materials have gained significant importance in the technology. These properties depend on the interaction of electromagnetic radiation with matter. This interaction is related to the wavelength and frequency of the radiation and material property like dielectric constant, refractive index, band gap values, etc. The tunable optical properties of materials have wide range of applications, ranging from biosensing to photovoltaics.

The plasma frequency (ω_p) is a characteristic frequency at which the material changes from metallic to dielectric, and this value is found as the zero-frequency equivalent of the real part of the dielectric function [70].

While visible region is specified by the energy range from 1.59 to 3.26 eV, ultraviolet region is specified by 3.26–12.4 eV [71]. The values of $\varepsilon_1(0)$ are in the order NaScSi (20 eV) > AgScSi (15.92 eV) [27] > LiScSi (12.5 eV) [30]. The summit of the real part of the dielectric function is in the IR region, and the peak of the imaginary part is found in the visible region (Fig. 6a, b). Negative values of $\varepsilon_1(\omega)$ show a metallic behavior in visible and UV regions. Consequently, the NaScSi compound can be said to be suitable for optical filters or shielding devices in different frequency regions. The static refractive index n (0), which is displayed in Fig. 6c, is found to be 4.52 and decreases with an increase in photon energy; after about 11 eV, it goes back to an increase. In the previous studies, the refractive index of KScSi [31], LiScSi [30], and AgScSi [27] compounds is 2.73, 4.6, and 4.51, respectively. Our values for the refractive index (4.52) are in good agreement with that of AgScSi (4.51) and are greater than those of other references [30, 31]. The extinction coefficient $k(x)$ is calculated and shown in Fig. 6d. The most distinct peak maxima of the extinction coefficient $k(x)$ are observed at about 2.49 at 1.5 eV. The maximum value of the extinction coefficient $k(x)$ of the AgScSi from previous studies is about 2.59 at 2.93 eV [27]. The energy loss function $L(\omega)$, another important factor defining the energy loss of a fast electron in a material, is presented in Fig. 6e. As can be seen from the figure, the highest energy loss occurs in the ultraviolet region. This main peak as it is called plasmon frequency (ω_p) is evaluated. These ω_p values are located at nearly 12.5. In the previous studies, the plasmon frequency of LiScSi and AgScSi structures is 12.5 and 15.92, respectively. The static reflectivity R (0) is displayed in Fig. 6f. As seen from the figure, it is the region with the most reflection in the UV region. Our value for the static refractive index at 0 GPa is in good agreement with results for LiScSi and AgScSi.

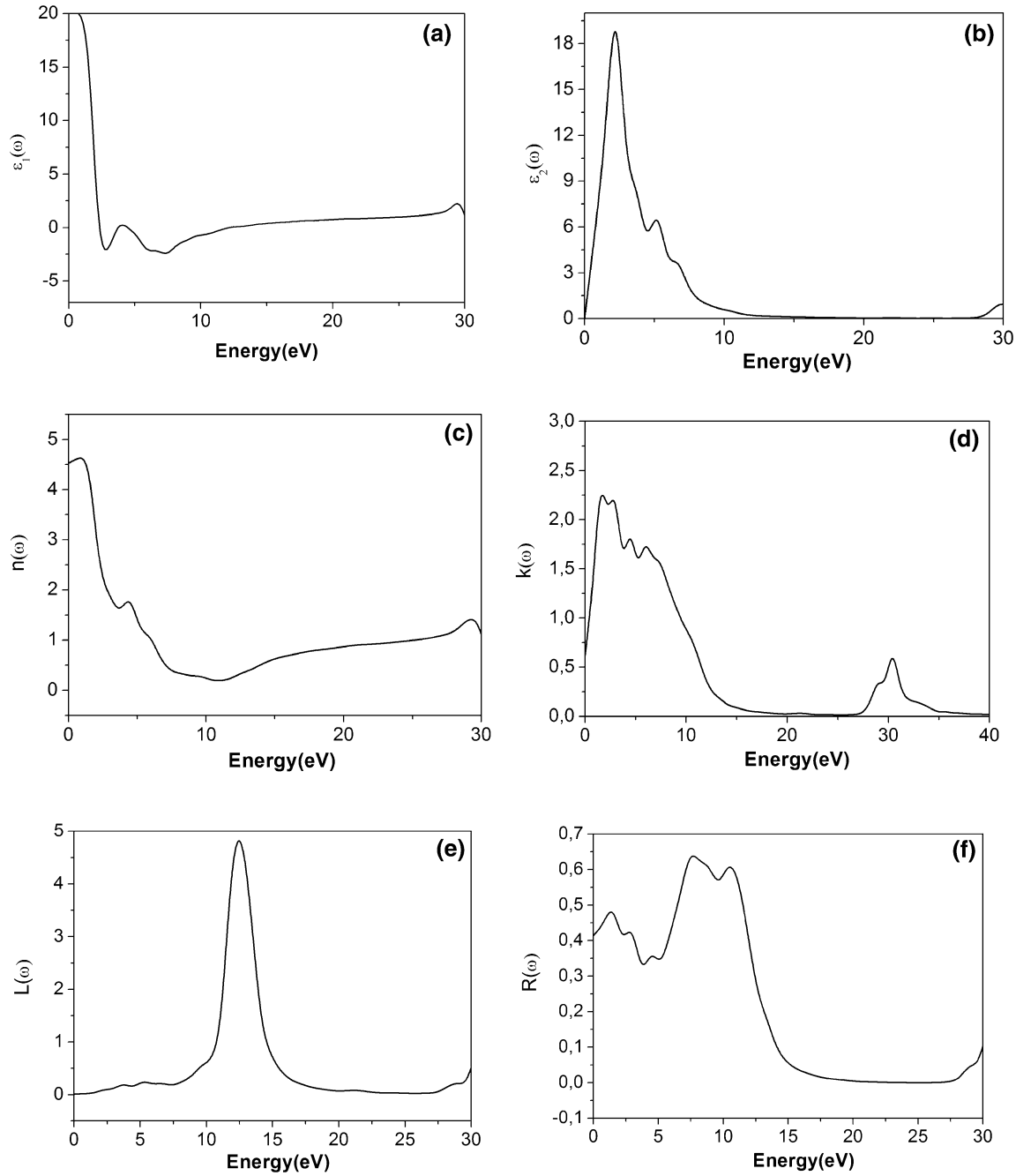


Fig. 6 Plot of (**a**) real parts of the dielectric function $\varepsilon_1(x)$, (**b**) imaginary parts of the dielectric function $\varepsilon_2(x)$, (**c**) refractive index $n(x)$, (**d**) extinction coefficient $k(x)$, (**e**) electron energy loss functional L (x), (**f**) reflectivity versus photon energy of NaScSi compound

4. Conclusion

Ab initio calculations have been used to study structural, mechanical, dynamic, thermodynamic, electronic, and optical properties of the NaScSi compound. First, we have optimized NaScSi in MgAgAs the structures, and using optimized unit cell we have determined elastic constants. The calculated elastic constants of NaScSi compound show the mechanical stability of the MgAgAs-type structure. Mechanical properties are determined using elastic constants. Pugh's ratio and Poisson's ratio indicate that this compound is ductile. Also, Cauchy relation confirms the ionic nature and ductile nature of this compound. Anisotropic ratio predicts that this compound is anisotropic. The

phonon dispersion curves show that compound is stable dynamically. Also, the heat capacity, entropy, and free energy of the NaScSi are calculated by using the phonon frequencies. It is found that S and C_v increase with increasing temperature, while F decreases with increasing temperature. Our electronic results indicate that NaScSi corresponds to a direct band (X–X) transition with a band gap of 0.619 eV which exhibits a semiconductor property. Furthermore, the optical properties of the NaScSi compound are found to vary according to photon energies and may be considered suitable for optoelectronic applications.

References

[1] F Heusler *Verh. Phys*. **5** 219 (1903)
[2] V Abdul Shukoor, M Sarwan and S Singh *Phys. B Condens. Matter* **547** 83 (2018)
[3] D M Hoat, J F Rivas-Silva and A Méndez Blas *J. Comput. Electron.* **17** 1470 (2018)
[4] T Graf, C Felser and S S Parkin *Prog. Solid State Chem*. **39** 1 (2011)
[5] A Candan, S Akbudak, M Özduran and A İyigör *Chin. J. Phys.* **56** 1772–1780 (2018)
[6] R L Zhang, L Damewood, C Y Fong, L H Yang, R W Peng and C Felser *AIP Adv*. **6** 115209 (2016)
[7] C Colinet, P Jund and J C Tédenac *Intermetallics* **46** 103 (2014)
[8] T Yang, J Cao and X Wang *Crystals* **8** 429 (2018)
[9] I Žutić, J Fabian and S D Sarma *Rev. Mod. Phys.* **76** 323 (2004)
[10] J D Boeck, W V Roy, Motsnyi, V Liu, Z Dessein and K Borghs *Thin Solid Films* **412** 3 (2002)
[11] T Graf, P Klaer, J Barth, B Balke, H J Elmers and C Felser *Scr. Mater.* **63** 1216 (2010).
[12] S Sakurada and N Shutoh *Appl. Phys. Lett.* **86** 082105 (2005).
[13] J R Sootsman, D Y Chung and M G Kanatzidis *Angew. Chem. Int. Ed.* **48** 8616 (2009)
[14] A Roy, J W Bennett, K M Rabe and D Vanderbilt *Phys. Rev. Lett.* **109** 037602 (2012)
[15] D Kieven, R Klenk, S Naghavi, C Felser and T Gruhn *Phys. Rev. B* **81** 075208 (2010)
[16] W Feng, D Xiao, Y Zhang and Y Yao *Phys. Rev. B* **82** 235121 (2010)
[17] S Chadov, X Qi, J Kubler, G H Fecher, C Felser and S C Zhang *Nat. Mater.* **9** 541 (2010)
[18] J Kubler *Phys. Rev. B* **67** 220403 (2003)
[19] VA Dinh, K Sato and H Katayama-Yoshida *J. Phys. Soc. Jpn*. **77** 014705 (2008)
[20] A Hirohata, J Sagar, L Lari, L Fleet and V Lazarov *Appl. Phys.* A **111** 423 (2013)
[21] A Hirohata and K Takanashi *J. Phys. D* **47** 193001 (2014)
[22] C Felser, L Wollmann, S Chadov, G H Fecher and S S P Parkin *APL Mater.* **3** 041518 (2015)
[23] C T Tanaka, J Nowak and J S Moodera *J. Appl. Phys.* **86** 6239 (1999)
[24] C Hordequin, J Nozieres and J Pierre *J. Magn. Magn. Mater.* **183** 225 (1998)
[25] C Felser, G H Fecher and B Balke *Angew. Chem. Int. Ed*. **46** 668 (2007)
[26] M Evecen and Y Öztekin Çiftci *J. Nanoelectron. Optoelectron.* **12** 100 (2017)
[27] I. Kars Durukan and Y Ö Çiftci *J. Electr. Mater.* **48** 4050 (2019)
[28] H Z Luo, H W Zhang, Z Y Zhu, L Ma, S F Xu, G H Wu, X X Zhu, C B Jiang and H B Xu J. *Appl. Phys*. **103** 1 (2008)
[29] W Schnelle, A Leithe-Jasper, H Rosner, R Cardoso-Gil, R Gumeniuk, D Trots, JA Mydosh and Y Grin *Phys. Rev. B* **77** 94421 (2008)
[30] Y O Ciftci and M Evecen *Phase Transit.* **91** 1206 (2018).
[31] S Kacimi, H Mehnane and A Zaoui *J. Alloys Compd.* **587** 451 (2014)
[32] M Ameri, A Touia, R Khenata, Y Al-Douri and H Baltache *Optic* **124** 570 (2013)
[33] A Missoum, T Seddik, G Murtaza, R Khenata, A Bouhemadou, Y Al-Douri, A Abdiche, H Meradji and H Baltache *Can. J. Phys*. **92** 1105 (2014)
[34] G Kresse and J Hafner *Phys. Rev. B* **47** 558 (1993)
[35] P Hohenberg and W Khon *Phys. Rev*. **136 B** 864 (1964)
[36] W Khon and L J Sham *Phys. Rev.* **140** A1133 (1965)
[37] G Kresse and J Hafner *Phys. Rev. B* **49** 14251 (1994)
[38] G Kresse and J Furthmuller *Comput. Mater. Sci*. **6** 15 (1996)
[39] G Kresse and J Furthmuller *Phys. Rev. B* **54** 11169 (1996)
[40] J P Perdew, S Burke and M Ernzerhof *Phys. Rev. Lett.* **77** 3865 (1996)
[41] H J Monkhorst and J D Pack *Phys. Rev. B* **13** 5188 (1976)
[42] A Toga, F Oba and I Tanaka *Phys. Rev. B* **78** 1 (2008)
[43] J B Gu, C J Wang, Y Cheng, L Zhang, L C Cai and G F Ji *Comput. Mater. Sci.* **96** 72–80 (2015)
[44] F Peng, H Z Fu and X L Cheng *Phys. B* **400** 83 (2007).
[45] F Peng, H Z Fu and X D Yang *Solid State Commun.* **145** 91 (2008)
[46] F Peng, H Z Fu, X D Yang *Phys. B* **403** 2851 (2008)
[47] M Glazer, G Burns, A N Glazer *Space Groups for Solid State Scientists* (New York: Academic Press) p 159 (1990)
[48] F D Murnaghan *Proc. Nat. Acad. Sci. USA* **30** 244 (1944)
[49] A Abdellaoui, M Ghaffour, M Bouslama, S Benalia, A Ouerdane, B Abidri and Y Monteil *J. Alloys Compd*. **487** 206 (2009)
[50] P Perdew and A Zunger *Phys. Rev. B* **23** 5048 (1981)
[51] C A Ponce, R A Casali and M A Caravaca *J. Phys. Condens. Matter.* **20** 045213/1-6 (2008)
[52] A Bouhemadou, R Khenata, M Chegaar and S Maabed *Phys. Lett. A* **371** 337 (2007)
[53] F Mouhat and F X Coudert *Phys. Rev. B* **90** 224104 (2014)
[54] D Wu, H Wang, L Wei, R Pan and B Y Tang J. *Magnes. Alloys* **2** 165 (2014)
[55] A Reuss, *Z. Angew. Math. Mech* **9** 49 (1929)
[56] R Hill *Proc. Phys. Soc.* **A 65** 349 (1952)
[57] W Voigt *Lehrburch der Kristallphysik* (New York: Johnson Reprint Corp.) p 32 (1966)
[58] X Q Chen, H Niu, D Li and Y Li *Intermetallics* **19** 1275 (2011)
[59] M Zhang, M Lu, Y Du, L Gao, C Lu and H Liu *J. Chem. Phys*. **140** 174505 (2014)
[60] L Vitos, P A Korzhavyi and B Johansson *Nat. Mater.* **2** 25 (2003)
[61] S F Pugh, *Philos. Magn.* **45** 823 (1954)
[62] S Ganeshan, S L Shang, H Zhang, Y Wang, M Mantina and Z K Liu *Intermetallics* **17** 313 (2009)
[63] D G Pettifor *Mater. Sci. Technol.* **8** 345 (1992)
[64] L Chaput, A Togo, I Tanaka and G Hug, *Phys. Rev. B* **84** 094302 (2011)
[65] J M Skelton, S C Parker, A Toga, I Tanaka and A Walsh *Phys. Rev. B* **89** (2014) 205203
[66] K Parlinski *PHONON software* (Poland: Cracow) (2005). https://wolf.ifj.edu.pl/phonon. Accessed 2 Jan 2008
[67] D Shirivastava and S P Sanyal *J. Alloys Comput*. **745** 240 (2018)
[68] M S Dresselhaus, M S Dresselhaus *Optical properties of solids* (New York: Academic Press) p 198 (1966)

[69] M N Baibich, J M Broto, A Fert, vDf Nguyen, F Peraff, P Etienne, G Creuzet, A Friederich and J Chazeles *Phys. Rev. Lett*. **61** 2472 (1993)

[70] M Ahmad, N Ullah, G Murtaza, R Khenata, S Bin Omran and A Bouhemadou *J. Magn. Magn. Mater.* **377** 204–210 (2015)

[71] R Majumder and Md M Hossain, *Comput. Condens. Matter* **21** e00402 1-6 (2019)

Publisher's Note Springer Nature remains neutral with regard to jurisdictional claims in published maps and institutional affiliations.